**Electronic Supplement to**

# From relative to absolute teleseismic travel-times: the Absolute Arrival-time Recovery Method (AARM)


## by A. Boyce, I.D. Bastow, S. Rondenay, R.D. Van der Hilst


## Additional Figures and Zip Archive

This electronic supplement presents further graphical output from testing of AARM on observed (data from SE Canada of *Boyce et. al., 2016)* and synthetic datasets. We also provide a zipped archive containing a copy of the AARM code. We include the code, plotting scripts and a detailed User Guide.

## Figures

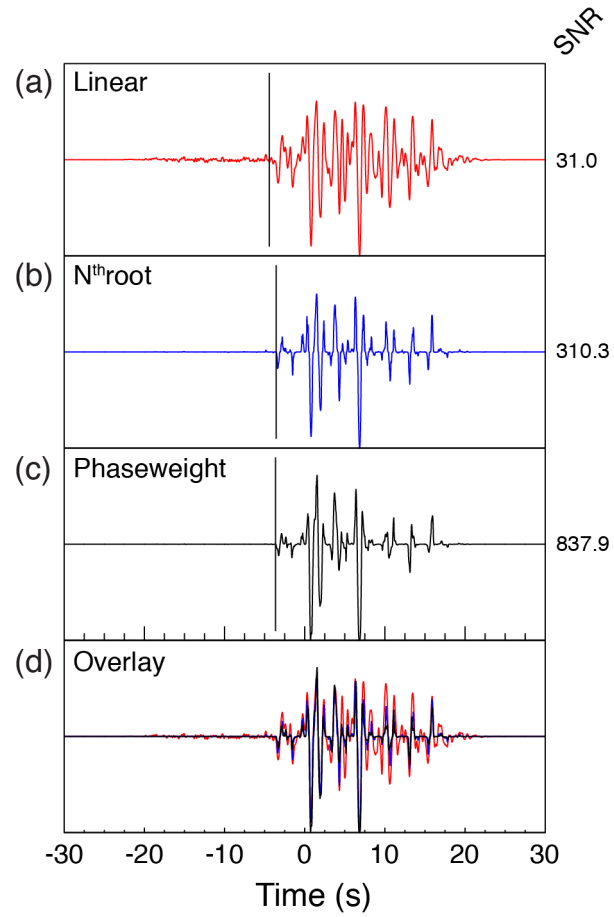

Figure S1. Figure to compare the pre-arrival noise suppression of linear (a), $n^{th}$root (b) and phaseweight (c) stacking for an example earthquake. (d) shows an overlay of the three stack types.

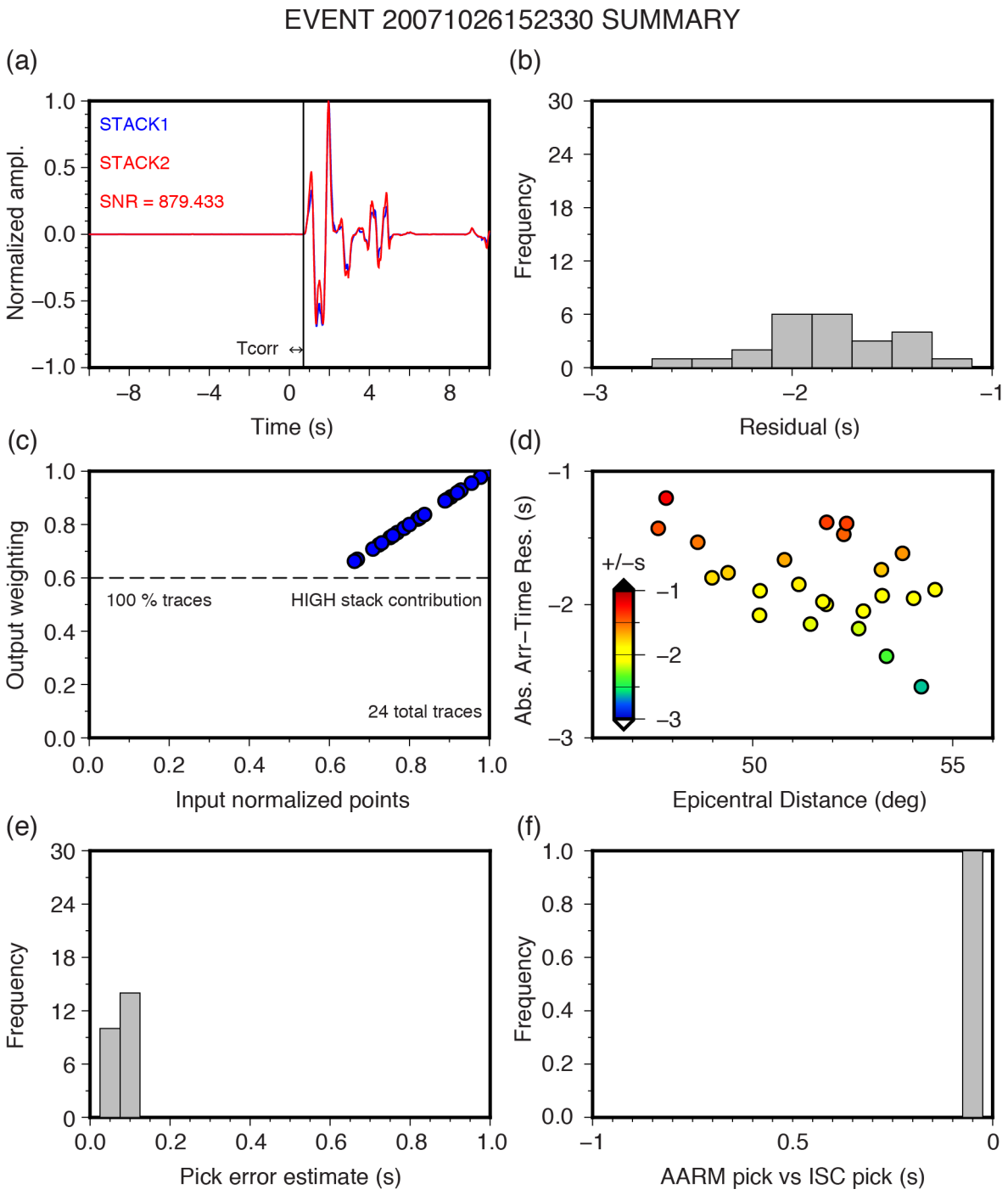


Figure S2. AARM output (using cross-correlation scheme) for an impulsive earthquake recorded by stations in SE Canada *(Boyce et. al., 2016)*. (a): Output stacks (blue primary

and red final) from alignment of traces. The correction time $T_{corr}$ is also shown. (b): Absolute arrival-time residual histogram. (c): Distribution of weights from cross-correlation of individual traces with the primary stack on the linear weighting scheme. (d): Absolute arrival-time residual distribution against epicentral distance. (e): The autocorrelation-derived estimate for picking error. (f): The difference between calculated absolute arrival-times from AARM and ISC picks where available (only one equivalent source-station pair exists for this event).

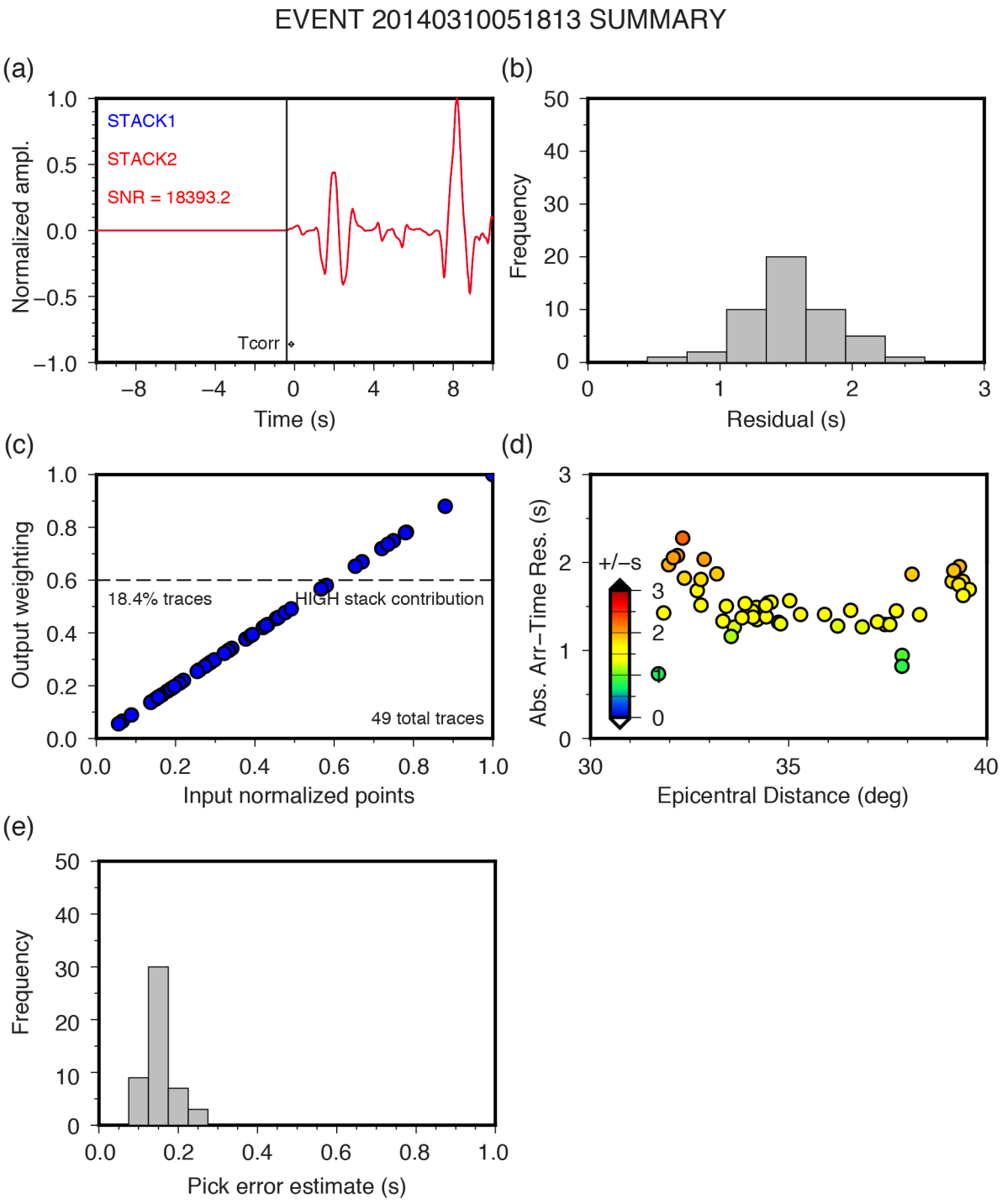


Figure S3. AARM output (using SNR scheme) for an emergent earthquake recorded by stations in SE Canada *(Boyce et. al., 2016)*, subplots are the same as Figure S2. Note that no corresponding ISC picks were available for this earthquake.

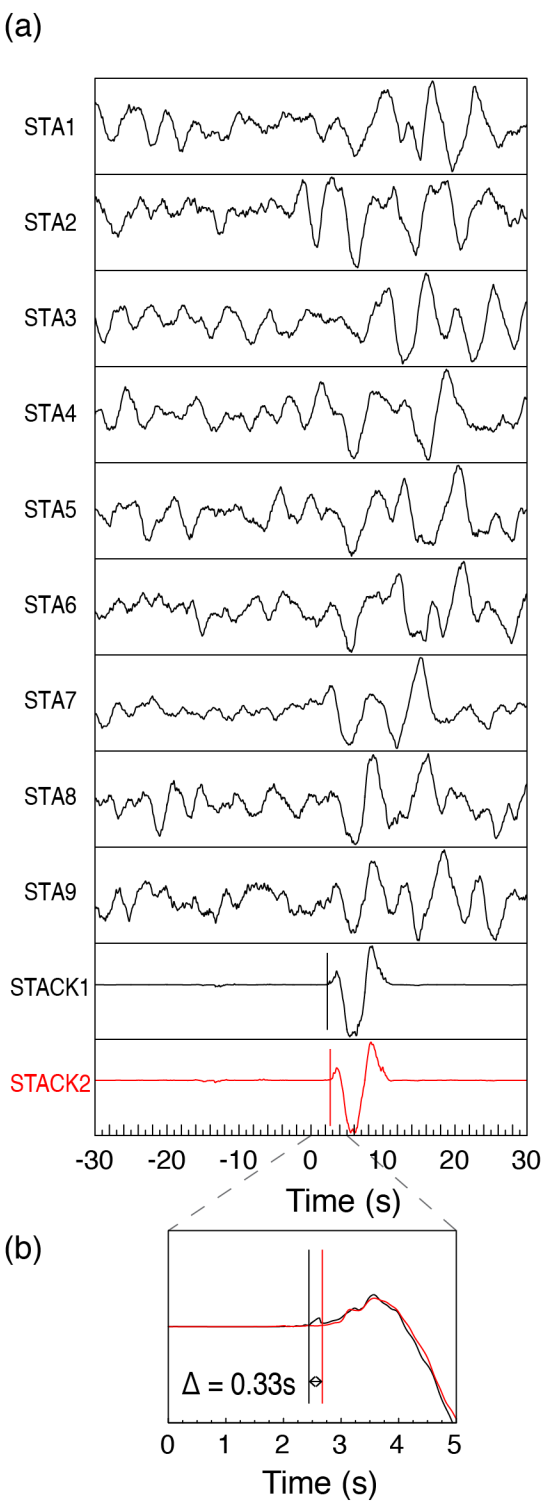


Figure S4. Figure to show nine variably noisy waveforms (STA 1-9) that contribute to the initial (stack1 - black) and final stack (stack2 - red) - (a). Vertical lines show manually picked arrival times. An expanded view of the stacks (b) shows the difference between the picks ( Δ ).

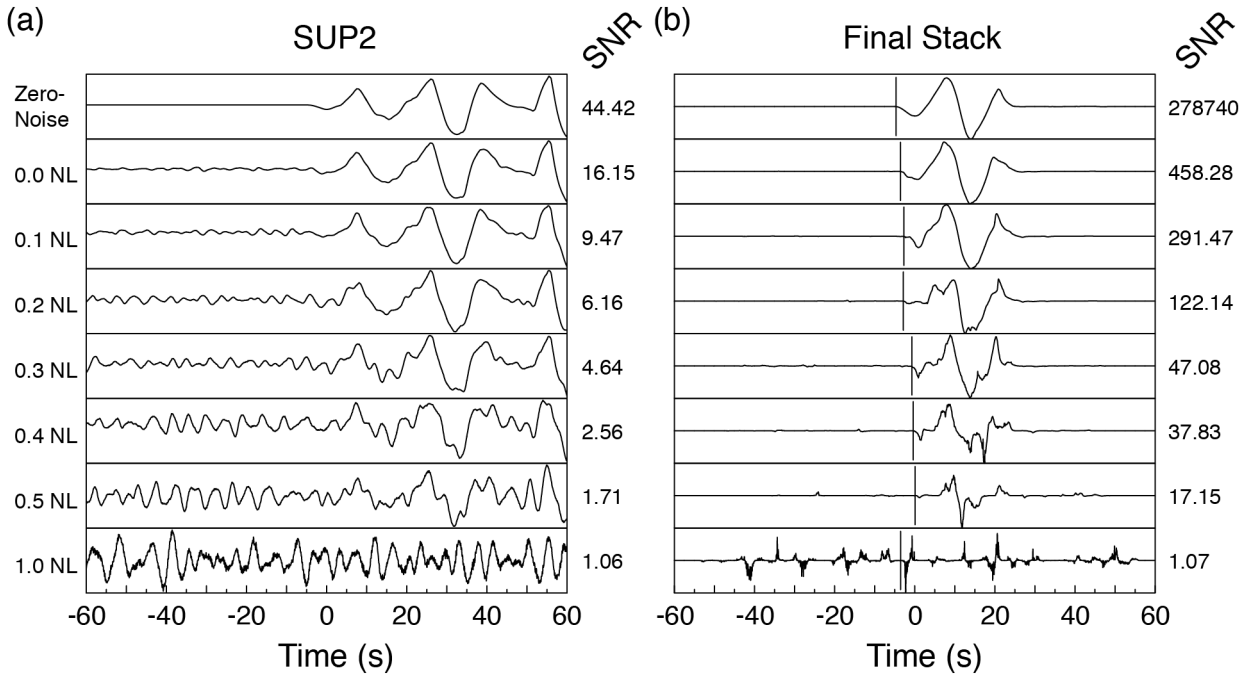


Figure S5. Plot to show how increasing levels of noise (Peterson et. al., 1993) affect individual traces at station SUP2 (a) and the final stack (b) for the S-wave synthetics (labels are the same as Figure 6 in the main manuscript – P-wave data).

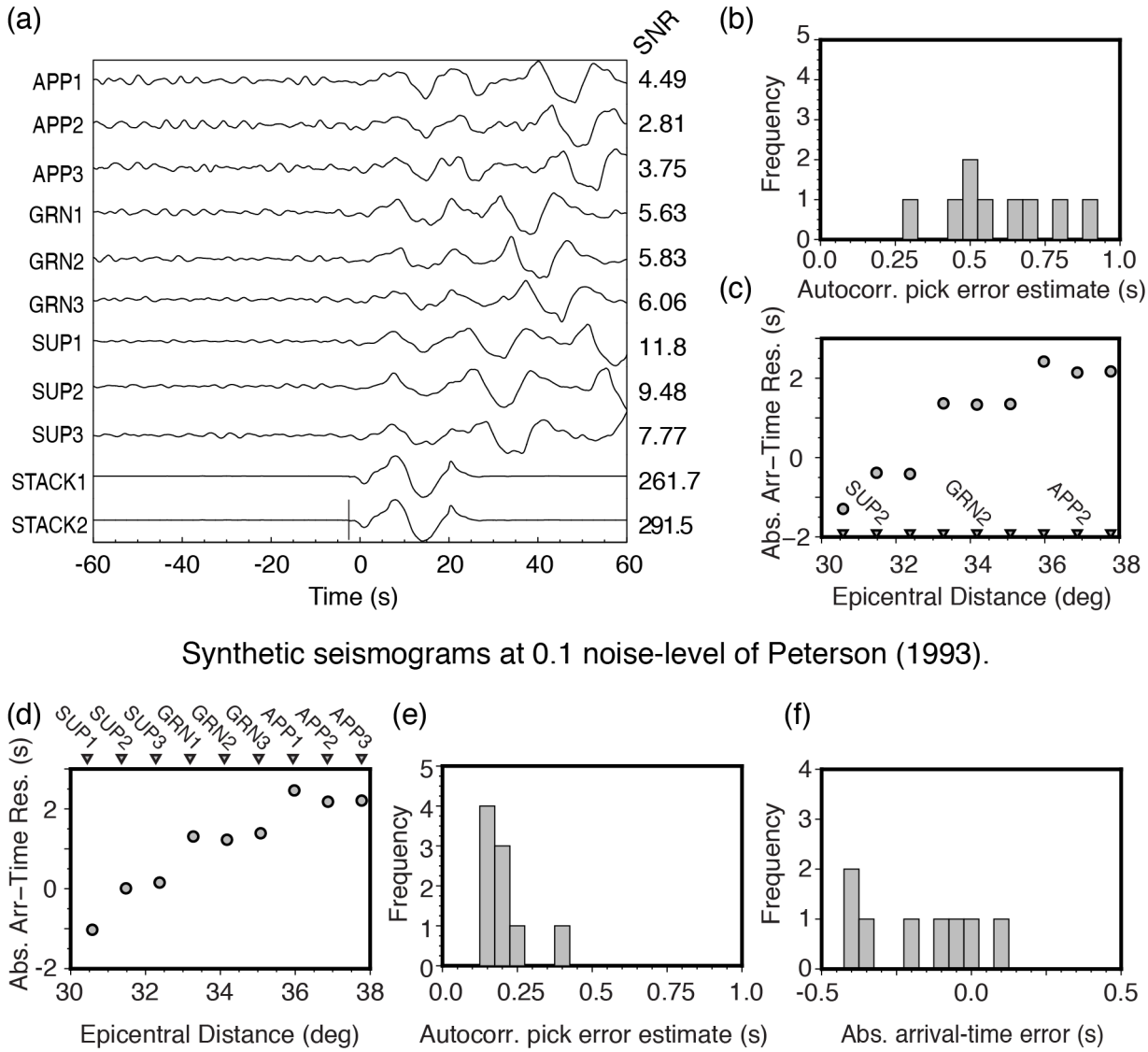


Figure S6. Figure to show results from S-wave synthetic testing, subplots are identical to Figure 7 in the main manuscript.

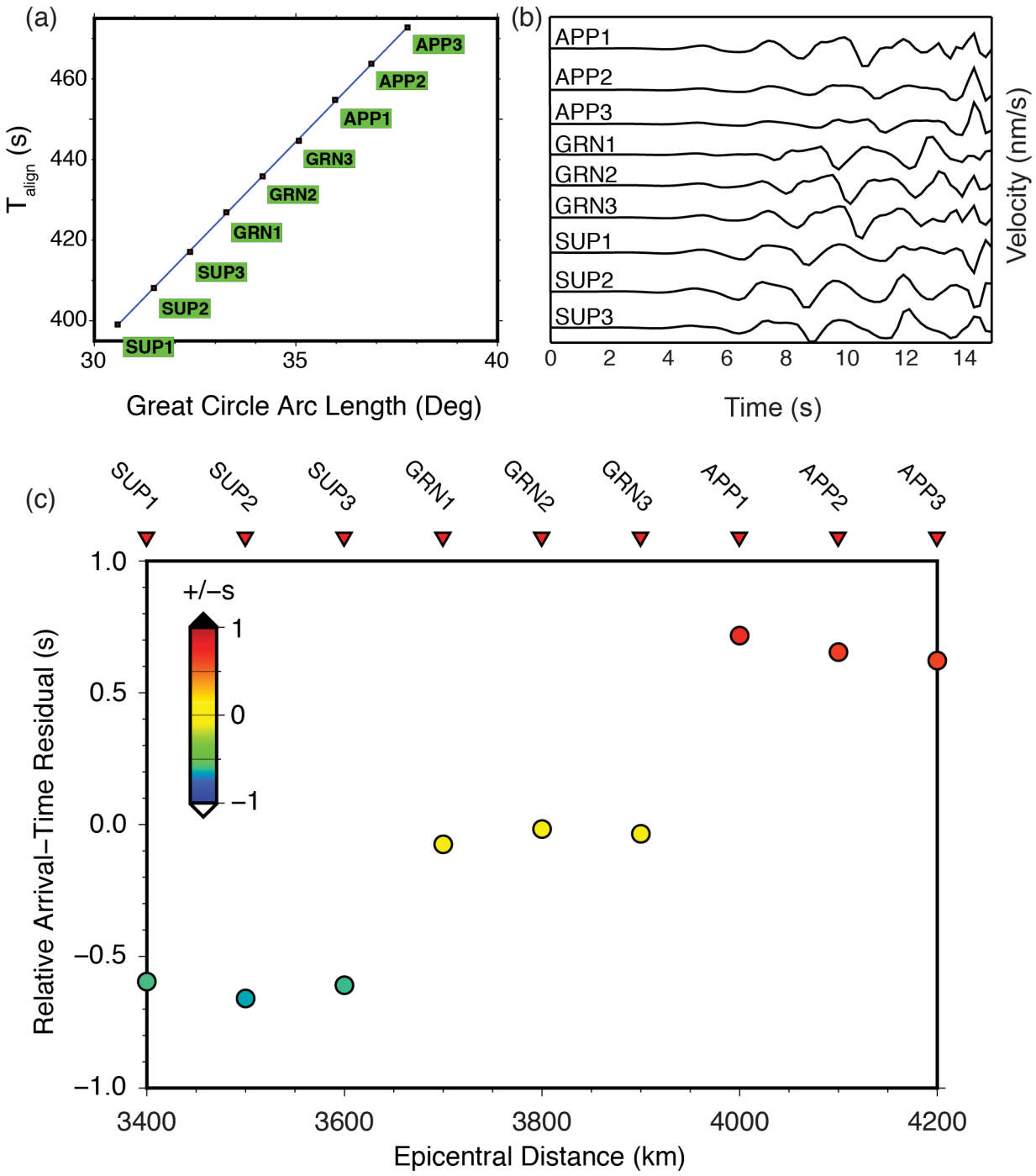


Figure S7. (a): Distribution of MCCC derived arrival-times $T_{align}$ *(VanDecar and Crosson, 1990)* with great circle arc length for the synthetic P-wave arrivals. (b): Filtered velocity seismograms aligned at 5 seconds on MCCC derived arrival-times. (c): The distribution of relative arrival-time residuals for the array of synthetic seismometers at increasing epicentral distance. The removal of the mean arrival-time for the array results in approximately zero residuals for central stations in this symmetric synthetic array.

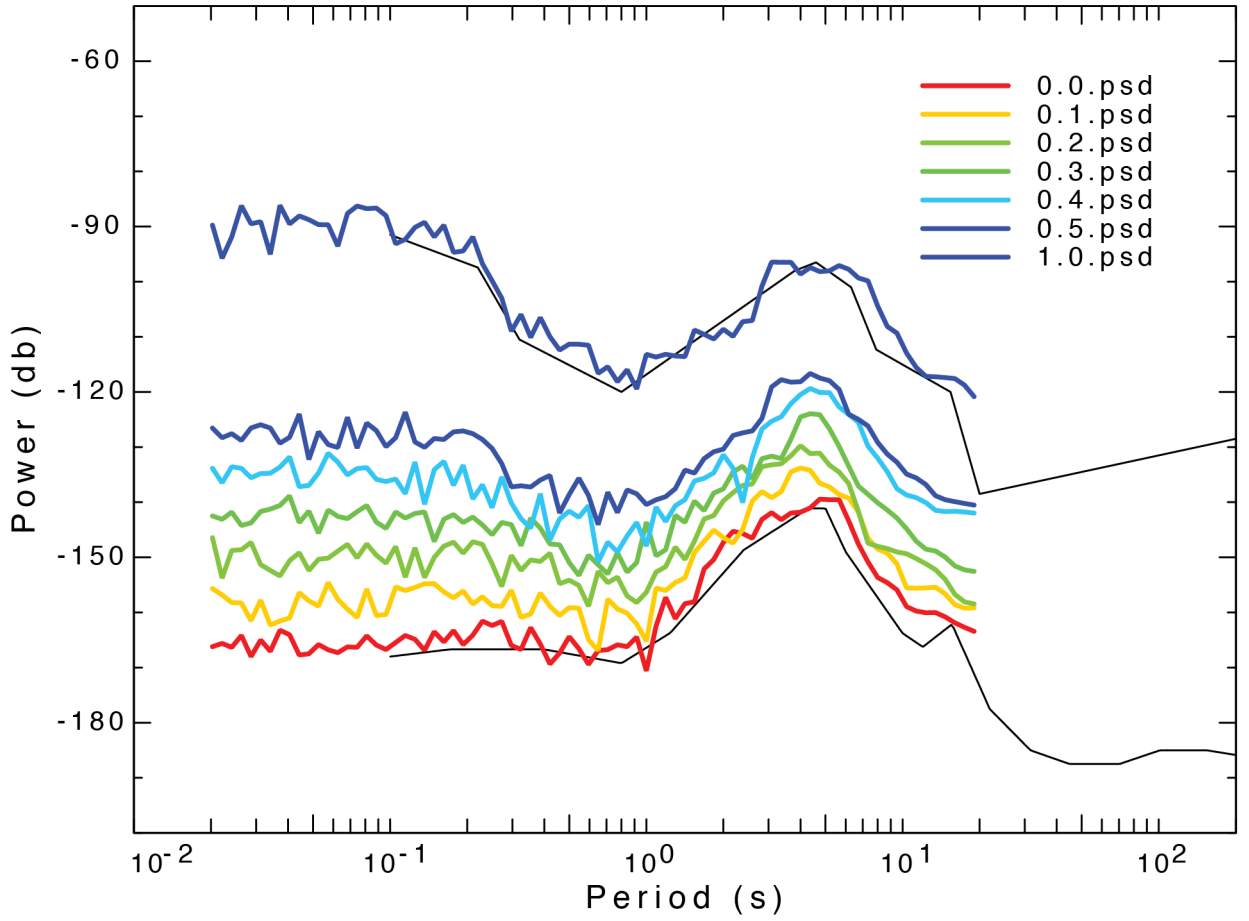


Figure S8. Modeled power spectra for teleseismic background noise models of *Peterson et. al., (1993)* varying between high (1.0) and low (0.0) extremes. These are used to add progressive levels of noise to synthetic seismograms. Black curves represent the upper and lower bound on observed noise.

# Zip Archive

Absolute_arrival-time_toolkit.tar.gz: Zip archive including AARM code, plotting scripts, example data and detailed user guide for AARM described in this paper.

References:

Boyce, A., I. D. Bastow, F. A. Darbyshire, A. G. Ellwood, A. Gilligan, V. Levin, and W. Menke (2016), Subduction beneath Laurentia modified the eastern North American cratonic edge: Evidence from P wave and S wave tomography, *J. Geophys. Res.,* **121(7)**, 5013–5030, doi:10.1002/ 2016JB012838, 2016JB012838.

Peterson, J., et al. (1993), Observations and modeling of seismic background noise, *U.S. Geol.*

*Surv. Open File Rep.*, pp. 93–322.

VanDecar, J., and R. Crosson (1990), Determination of teleseismic relative phase arrival times using multi-channel cross-correlation and least squares, *Bull. Seis. Soc. Am.,* **80(1)**, 150–169.